PHYSICAL REVIEW B VOLUME 27, NUMBER 6 15 MARCH 1983

Angle-resolved-photoemission study of the Cr(100) surface

G. Gewinner, J. C. Peruchetti, and A. Jaéglé
Laboratoire de Physique et de Spectroscopie Electronique, Institut des Sciences Exactes et Appliquées, Université de Haute Alsace, F-68093 Mulhouse Cedex, France

R. Pinchaux
Laboratoire pour l'Utilisation du Rayonnement Electromagnétique, Université Paris—Sud, F-91405 Orsay, France
(Received 28 June 1982; revised manuscript received 13 October 1982)

Normal and off-normal angle-resolved-photoemission data for Cr(100) are reported. Assuming a free-electron-like final-state band, bulk energy-band dispersions along the Γ-Δ-H, H-G-N, and N-D-P symmetry lines are determined. Measured critical-point binding energies are 0.95 (Γ_{25}'), 2.0 (N_2,P_4), 3.40 (H_{12}), and 4.0 eV (N_1). Standard self-consistent band-structure calculations predict larger d-band widths than those measured (typically by 20% at N_2). Evidence for a prominent surface state with a binding energy of 0.65 eV at the $\bar{\Gamma}$ point of the surface Brillouin zone is found for clean Cr(100).

I. INTRODUCTION

There is considerable interest in understanding the electronic structure of transition metals. Extensive and increasingly realistic theoretical one-electron band calculations can now be compared directly with angle-resolved-photoemission measurements. Much recent experimental investigation concerns[1-4] Ni and Cu.[5-7] The result of all this work is that whereas Cu works quite well, a narrowing of about 30% of the d bandwidth and a reduction of the exchange splitting are observed in the case of Ni. In addition the photoemission spectra of Ni show an energy level $\simeq$6 eV below the Fermi energy which is attributed to the excitation of a virtual two-hole bound state in the d band.[8] Hence, extensive theoretical effort has been expanded to explain these discrepancies on the basis of correlation effects within the unfilled narrow d band.[9-20] Obviously, it is interesting to extend the work in this area to related metals. Recent experiments[21,22] on Co and Fe indicate that the band calculations describe these metals much better than Ni, but similar problems are apparently encountered.

We report here results from a photoemission investigation of a Cr(100) surface, concerning mainly the bulk electronic structure. A previous photoemission study for mapping out the bulk energy bands of Cr has been reported by Johansson *et al.*[23] These authors investigated normal emission from a Cr(110) surface below and above the Néel temperature ($T_N = 312$ K) in an attempt to observe spectroscopic effects of the magnetic-phase transition. Reasonable agreement was found with the antiferromagnetic bands of Asano and Yamashita[24] along the Γ-Σ-N direction for the data collected at 230 K. Chromium crystallizes in a body-centered-cubic (bcc) structure. The antiferromagnetic state is described by a spin-density wave with a wave vector Q close to $(2\pi/a)(1,0,0)$. The transition from paramagnetic to antiferromagnetic chromium is accompanied by a reduction of the symmetry. Hence states of wave vector $k \pm Q$, $k \pm 2Q$, etc. are mixed with a given Bloch state k. Small gaps are introduced at points where the states to be mixed are nearly degenerate. Calculations assuming perfect $[Q = (2\pi/a)(1,0,0)]$ antiferromagnetic Cr show gaps of typically 0.2 eV.[24,25] Thus a gross picture of the band structure of perfect antiferromagnetic Cr is obtained when the dispersion curves for paramagnetic Cr are drawn in the reduced zone, i.e., the simple-cubic Brillouin zone for the CsCl-type lattice.[24] Most of the band-structure calculations reported so far concern the paramagnetic state.[24,26-31]

II. EXPERIMENTAL PROCEDURE

Experiments on both clean and nitrogen-covered Cr(100) are reported. Measurements on the clean sample were carried out utilizing a Vacuum Generator ADES 400 electron spectrometer and the photoelectrons were produced by radiation from a resonance lamp. Experiments on a nitrogen-covered surface were performed at the Laboratoire pour l'Utilisation du Rayonnement Electromagnétique

(LURE) using synchrotron radiation from the Anneau de Collision d'Orsay (ACO) (Orsay storage ring). Though the latter experiments were primarily designed for the study of the surface electronic structure, results of interest concerning the bulk band structure were also obtained. In both experiments an electron energy analyzer can be rotated around the sample in the horizontal plane. Low-energy electron diffraction is used to select the plane of emission by rotating the sample around its normal. The angular resolution is about $\pm 2°$ and the energy resolution (electron + photon) was kept at $\simeq 0.2$ eV.

The chromium single crystals were spark-cut after orientation $\pm\frac{1}{2}°$ and mechanically and electrolytically polished using standard techniques. The nitrogen-covered surface is a Cr(100)-(1×1)-N structure which is prepared as described previously.[32] A clean Cr(100)-(1×1) surface was obtained after prolonged argon ion etching and simultaneous heating at 600–800 °C. This lengthy procedure reduces the amount of bulk impurities (C, N, and S), which diffuse to the surface during annealing, to a negligible level. We have previously suggested that clean Cr(100) may be reconstructed in a $c(2\times2)$ superstructure.[33] Actually, a small amount of impurities (C, N, O, or S) must be present to observe this superstructure. This problem is discussed elsewhere.[34,35] The spectra reported here referred to the clean surface correspond to a Cr(100)-(1×1) surface structure. Owing to the very rapid adsorption of CO from residual atmosphere ($P\simeq 5\times10^{-11}$ Torr) a standard cleaning cycle (ion etching followed by annealing at 400 °C) was repeated every 1–2 h.

Direct interpretation of the angle-resolved energy distribution curves (EDC's) is based on symmetry-selection rules associated with electric dipole transitions. Owing to the translation symmetry parallel to the crystal surface, components of the wave vector parallel to the surface $k_{||}$ are conserved. Hence $k_{||}$ for the initial state is readily determined from the kinetic energy and exit angle of the emitted electron. In the direct-transition model, which describes emission from bulk states, the perpendicular component of the wave vector $k_\perp$ can be determined if the dispersion of the final- (or initial-) state band is known and several studies[2,5,6,36] have shown that a free-electron final-state band often works quite well. Simple arguments in favor of this approximation may be given if the final-state energy is not too low.[37] Assuming that primary cone emission is predominant,[38,39] simple kinematic equations can be derived from energy and momentum conservation:

$$k_{||}=0.513(\hbar\omega+E-\Phi)^{1/2}\sin\theta\ , \tag{1}$$

$$k_\perp=0.513\,|\,(\hbar\omega+E-\Phi)\cos^2\theta+V_0\,|^{1/2}\ , \tag{2}$$

where k (Å^{-1}) is the wave vector in the extended zone scheme, $\hbar\omega$ (eV) the photon energy, E (eV) the initial-state energy referred to the Fermi level, and θ the polar angle of emission. The value of the crystal inner potential $V_0=10.8$ eV, that is used, is approximately the sum of the Fermi energy and the work function Φ. This procedure seems reasonable as a first approximation. Johansson *et al.*[23] have used a somewhat lower value ($\simeq 9.8$ eV) resulting from a fit of the free-electron parabola with calculated bands[30] in the appropriate energy range (15–25 eV). However, the accuracy of these band calculations has been questioned.[31] Actually, the results are not very sensitive to a small adjustment ($\simeq 1$ eV) of V_0.

Since the photoemission data are collected at room temperature, i.e., just below T_N, they are, in principle, to be compared with calculations concerning the antiferromagnetic state. However, the effects on the dispersion curves $E(k)$, due to the magnetic state, are rather small[24] and generally less than the variations in the $E(k)$ among the different calculations for either perfect antiferromagnetic or paramagnetic Cr. Thus, since most of the theoretical works concern the paramagnetic state the data are compared with the numerous band calculations for paramagnetic Cr. Also, the bcc Brillouin zone is used in the analysis of the photoemission spectra rather than the reduced simple cubic zone corresponding to the perfect antiferromagnetic state. Actually, it will appear below that the prominant features in the photoemission spectra collected at room temperature can be accounted for by direct transitions in the bcc rather than the reduced Brillouin zone.

All the data are taken in an azimuth which corresponds to one of the two mirror planes of the (100) surface. Figure 1 displays cross-sectional cuts through the (repeated) Brillouin zones in these planes normal to the surface. Within the approximation of free-electron dispersion in the final band, the points probed in k space at constant final energy for different polar angles are located on circles. Using Eq. (1), $k_{||}$ can be plotted on the vertical axis. This permits a quick determination of $\vec{k}$ knowing the final-state energy.

III. RESULTS AND DISCUSSION

Figure 2 shows a series of selected EDC's collected from the clean surface at normal emission and $\hbar\omega=16.8$ (NeI), 21.2 (HeI), and 40.8 eV (HeII), which probe bulk states along the Γ-Δ-H direction of the Brillouin zone. The peak at -0.65 eV shows no dispersion with photon energy. Furthermore, it can be seen from the dashed curve recorded from a surface containing $\sim\frac{1}{3}$ of a monolayer of nitrogen

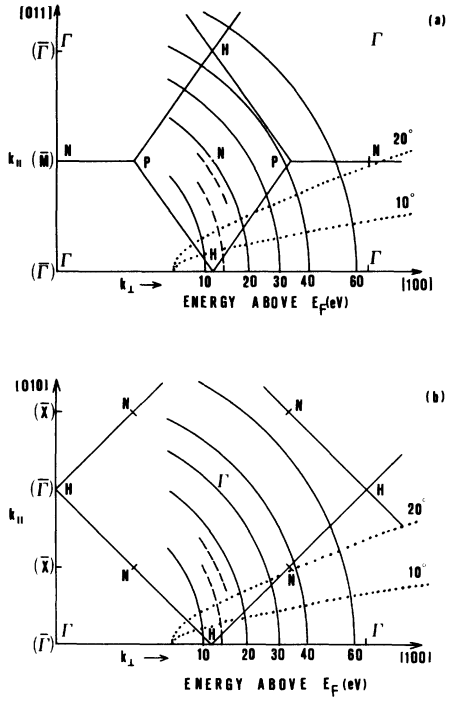

FIG. 1. Cuts through the repeated Brillouin zones of Cr. The horizontal axis is $k_\perp$ relative to the (100) surface: in (a) $\vec{k}_{||}||[011]$ and in (b) $\vec{k}_{||}||[010]$. The dashed lines show the $\vec{k}$ location at off-normal photoemission for $\hbar\omega=16.8$ eV and $0°\leq\theta\leq45°$ and for $\hbar\omega=21.2$ eV and $25°\leq\theta\leq50°$ with the initial-state energy corresponding to the lower-energy band. The circles are contours of constant final energy in the free-electron final-state band approximation. The dotted lines show contours of constant polar angle of emission θ. Symmetry points of the surface Brillouin zone are shown in parentheses.

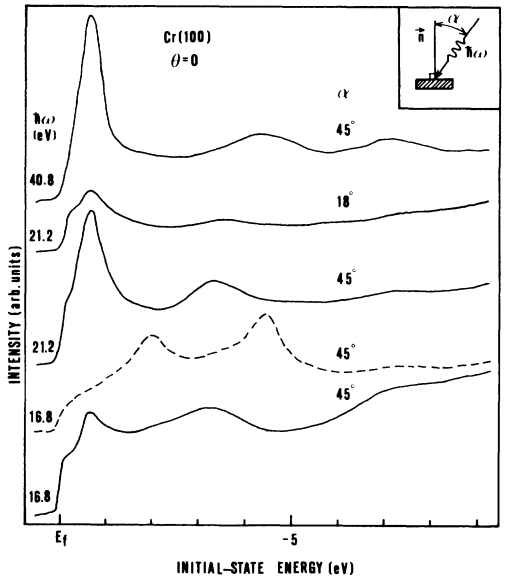

FIG. 2. Photoemission energy distributions for normal emission from Cr(100). Solid lines represent spectra from the clean sample. α is the incidence angle of light. The dashed curve corresponds to a Cr(100) surface containing $\simeq\frac{1}{3}$ of a monolayer of nitrogen.

that this feature is very sensitive to surface contamination. At normal emission from the (100) surface only bulk (surface) states of Δ_1 ($\bar{\Gamma}_1$) or Δ_5 ($\bar{\Gamma}_5$) symmetry can contribute to photoemission.[40] Δ_1 states are excited by the component of the vector potential normal to the surface. This component can be varied in our experiment by changing the angle of incidence of the light α. The spectra at $\hbar\omega=21.2$ eV for $\alpha=18°$ and $\alpha=45°$ show that the structures at -0.65 and -3.4 eV have mainly Δ_1 character. The solid lines in Fig. 3 illustrate the calculated bulk band structure of paramagnetic chromium from Ref. 24. It can be seen that there are no bulk states of Δ_1 symmetry which may account for the peak at -0.65 eV. Hence it reflects emission from a surface state in the $\bar{\Gamma}_1$ symmetry gap of the projection of the bulk band structure. In fact, this feature is quite similar to the well-known surface state ob-

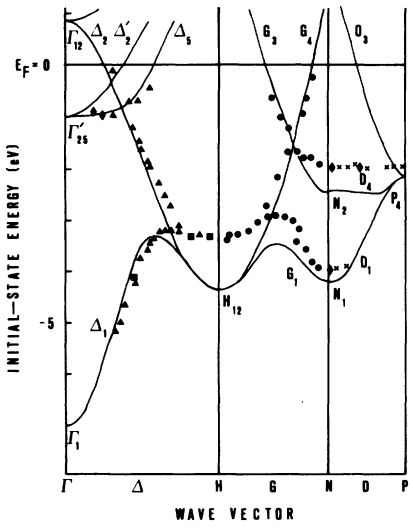

FIG. 3. Energy bands of Cr along the ΓH, HN, and NP symmetry lines. Solid curves are theoretical dispersion curves for paramagnetic Cr from Ref. 24. Squares are experimental points from normal-emission spectra; triangles, circles, crosses, and diamonds are experimental points from off-normal—emission spectra.

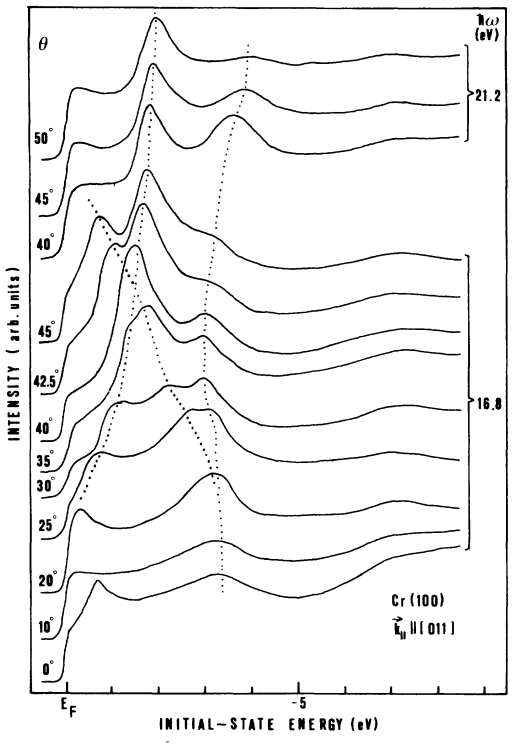

FIG. 4. Off-normal—emission spectra from clean Cr(100) for $\vec{k}_{||}||[011]$ corresponding to k points on the dashed lines in Fig. 1(a). The photon energy $\hbar\omega$ and polar emission angle θ are indicated. Dotted curves indicate peaks due to primary cone emission. The light was incident at 45° with respect to the surface normal.

served in field emission and photoemission from Mo(100) and W(100) surfaces.[41] The structure at $\simeq -7$ eV does not disperse with photon energy. A one-dimensional density-of-states peak arising from the lower sp band around Γ_1 could explain this feature. However, this is inconsistent with the fact that the same structure is still observed in the off-normal spectra of Fig. 4. An interpretation in terms of a multielectron satellite has been proposed for a similar structure observed at -6 eV on Cr(110).[23,42] We now consider the feature at -3.4 (-4.2) eV for $\hbar\omega = 16.8$ or 21.2 (40.8) eV. It has Δ_1 symmetry and disperses with photon energy. Hence, it may be attributed to direct transitions from the lower bulk band of Δ_1 symmetry. With the use of the formulas (1) and (2) binding energies corresponding to bulk electronic transitions are plotted on the band structure on Fig. 3. Experimental results determined from the spectra of Fig. 1 are shown as squares.

At an arbitrary photon energy and polar angle of emission, the EDC probes a general point in k space with no particular symmetry. For Cr(100) it appears that, according to Eqs. (1) and (2), off-normal emission spectra with $\vec{k}_{||}||[011]$, i.e., emission in a $(0\bar{1}1)$ mirror plane, probe points very close to the HN symmetry line for $\hbar\omega = 16.8$ eV and $0° \lesssim \theta \lesssim 45°$ or $\hbar\omega = 21.2$ eV and $25° \lesssim \theta \lesssim 50°$. Typical spectra recorded in these conditions from the clean surface are presented in Fig. 4. The relevant points in k space, calculated for the high-binding-energy feature corresponding to the lower G_1 band, are shown by the dashed lines in Fig. 1(a). The repeated zone scheme shown in this figure corresponds to the $(0\bar{1}1)$ or ΓHP mirror plane. A small deviation from HN has little effect on the measured energy-band dispersions $E(k)$ since k is broadened by lifetime effects in the final state (typically $\Delta k/k \simeq 10\%$) and the band dispersions are stationary for small deviations normal to the symmetry line. Only the data corresponding to deviations (Δk) less than one-tenth the distance ΓH are considered to fairly represent the symmetry line. Experimental $E(k)$ determined in this way are shown as circles in Fig. 3. Using a similar procedure, experimental band dispersions are obtained along ΓH from off-normal spectra with $\vec{k}_{||}||[010]$, i.e., emission in (001) mirror plane [Fig. 1(b)] with $\hbar\omega = 16.8$ eV and $0 \lesssim \theta \lesssim 45°$ or $\hbar\omega = 21.2$ eV and $25° \lesssim \theta \lesssim 50°$. The relevant data are shown as triangles in Fig. 3.

With a few exceptions (mainly for $\theta \lesssim 10°$), the prominent peaks in the EDC's show no particular sensitivity to surface contamination and can be considered to represent primary cone emission from bulk states. As can be seen in Fig. 3, it is remarkable that the spectra show emission from all the predicted bands. The agreement with calculated bands is fairly good for Δ_5 and the upper parts of Δ_2, G_3, and G_4. This suggests that the technique locating the initial states in k space, based on direct transitions to a final state with a free-electron dispersion, works rather well. Yet, substantial discrepancies between calculated and measured $E(k)$ exist, particularly in the lower part of the bands, where the measured binding energies are always lower than calculated.

Let us consider two possible explanations of this disagreement. Firstly, the uncertainty about the position in k space which approximately coincides with the appropriate symmetry line might cause deviations from the calculations along that symmetry line. The deviation at H_{12} and N_2, which results from a change in wave vector k in the direction normal to the G line, can be estimated directly from the calculated bands along the Δ and D lines. There is no binding-energy change at N_2 since the D_4 band is quite flat. The deviation at H_{12} is 0.15 eV for Δk equal to one-tenth the distance along ΓH, which is

much less than the observed discrepancy (~ 0.8 eV). Hence, since the strongest discrepancies occur near H and N, it appears that the agreement between theory and experiment would not be substantially improved if a more rigorous procedure had been used, involving a comparison of the experimental data with the bands determined off the symmetry lines by means of an interpolation scheme.

The second possible reason for the disagreement between theory and experiment is that the approximation of a free-electron final band is too crude, especially when k comes close to the zone boundary near H and N and that the use of more realistic final bands would reconcile our data with the calculations. First, let us consider the results around H. No calculations of final bands in the appropriate energy range ($E > 10$ eV) along ΓH have been published. Nevertheless it can be seen from Ref. 31 and from calculations[43] for Mo, which has a similar band structure, that there are no Bloch states of Δ_1 symmetry for $10 \lesssim E \lesssim 16$ eV. This would imply that the feature at -3.4 eV in the spectrum at normal emission and $\hbar\omega = 16.8$ eV reflects emission via surface-evanescent final states and represents a peak in the one-dimensional density of states along ΓH. Hence, a look at the calculated band structure in Fig. 3 shows that either two peaks around -3.4 and -4.3 eV (or at least a broad peak at an intermediate energy), reflecting the extrema of the Δ_1 band near the middle point of the symmetry line ΓH and near H, should be seen, or the H_{12} state has indeed a lower-binding energy than calculated as shown by the experimental data of Fig. 3. In this respect we note also that the present determination of H_{12} is consistent with the results of Ref. 23 as well as with x-ray photoemission work which places this critical point at[44] -3.5 eV rather than at the calculated position about -4.2 eV. Actually, previous work has shown that the free-electron final-state band approximation is applicable near the zone boundaries as well as at general points, mainly because of lifetime broadening in the final state.[37] Nevertheless, it appears that further investigations are necessary to substantiate (or disprove) the free-electron final-state band hypothesis in the vicinity of H_{12} for Cr. For instance, either accurate calculated final-state bands are used once they become available or a method independent of any assumption about the final states is employed.

We show now that a similar deficiency cannot be invoked to explain the data concerning the critical points N_1 and N_2 where similar discrepancies are encountered and conclude that at least in that case the observed binding energies are actually lower than calculated. The following independent measurements strongly support both the data around N

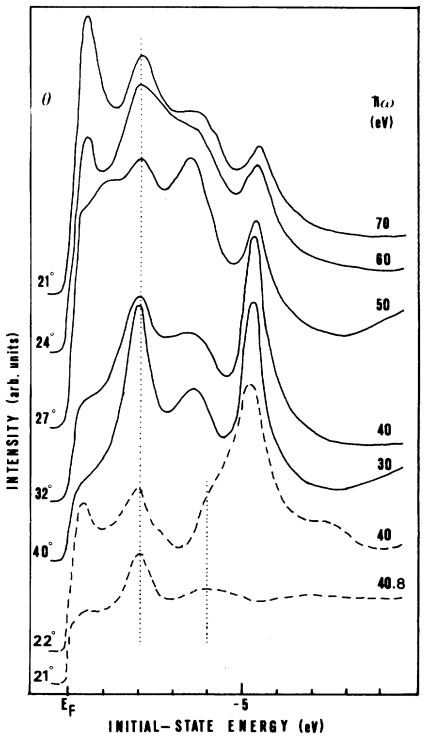

FIG. 5. Off-normal emission spectra from Cr(100). Dashed lines are spectra with $\vec{k}_{\parallel} \| [010]$, probing the symmetry point N: The lower spectrum is from clean Cr(100) and the upper spectrum from Cr(100)-(1×1)-N. Solid lines represent spectra from Cr(100)-(1×1)-N with $\vec{k}_{\parallel} \| [011]$ and with $k_{\parallel}$ held fixed at point $\bar{M}$. The photon energy and polar emission angle are indicated. Dotted lines indicate peaks due to emission from bulk states. The other features in the spectra from Cr(100)-(1×1)-N are due to nitrogen-induced surface states at the $\bar{X}$ (for $\vec{k}_{\parallel} \| [010]$) or $\bar{M}$ (for $\vec{k}_{\parallel} \| [011]$) points of the surface Brillouin zone and are not discussed here (see Ref. 32).

and the validity of the free-electron final-state band approximation in this region of k space.

The lower dashed spectrum in Fig. 5 is collected from the clean surface at $\hbar\omega = 40.8$ eV and $\theta = 21°$ in the (001) or ΓHN plane. It can be seen from Fig. 1(b) that it probes points very close to N. Two peaks at -2.0 and -4.0 eV can be seen which agree very well with the binding energies of the N_2 and N_1 states determined previously from emission in the $(0\bar{1}1)$ plane. Further evidence that these peaks represent indeed emission from bulk rather than surface states comes from the upper dashed spectrum in Fig. 5 which is collected from a Cr(100)-(1×1)-N surface at $\hbar\omega = 40$ eV and $\theta = 22°$ in the (001) mirror plane. Again this spectrum probes N and in addi-

tion to peaks derived from the nitrogen orbitals it shows clearly the emission from the N_2 and N_1 bulk states at -2.0 and -4.0 eV, respectively. These and a few similar results at other points of k space are shown in Fig. 3 as diamonds. Data coming from independent measurements always agree very well. An important observation is that weak peaks at -2.0 and -4.0 eV are generally present in any spectrum corresponding to the $\bar{X}$ point of the surface Brillouin zone, i.e., with $k_{||}$ at the middle of the symmetry line ΓH. These spectra are obtained by varying the photon energy and polar angle in such a way that $k_{||}$ remains constant. Both features become stronger when the direct-transition condition is fulfilled as in the case of the dashed spectra in Fig. 5. This implies that both weak peaks correspond to maxima in the one-dimensional density of states corresponding to the critical points N_1 and N_2. These peaks are the result of either indirect transitions or secondary cone—surface umklapp processes.[39] Thus, this result determines the critical points N_1 and N_2 independent of any assumption about the final states.

Finally we discuss spectra which determine the dispersion of the D_4 band along PN. Figure 5 shows as solid lines, typical EDC's collected in the (011) plane from a Cr(100)-(1×1)-N surface using synchrotron radiation. The photon energy is varied from 30 to 70 eV and the polar angle is adjusted according to Eq. (1) such that with $k_{||}$ at point $\bar{M}$ it can be seen from Fig. 1(a) that the possible bulk transitions originate from the PN symmetry line. On the basis of previous studies,[32] it appears that the prominant peak at -2.0 eV which shows essentially no dispersion cannot be assigned to emission from adsorbate-induced surface states. Therefore, interpreting it as the result of direct transitions from bulk states yields the experimental $E(k)$ shown as crosses in Fig. 3. Excellent agreement is found with the binding energy of N_2 already determined independently. Clearly, we observe here emission from the flat D_4 band connecting N_2 and P_4. Emission from D_1 can also be seen in the spectra probing points close to N where interference with the emission from N $2p$—derived surface states does not occur. Again the measured bands are shifted upwards in comparison with the calculations. Let us point out that since the D_4 band is quite flat the determination of $k_\perp$, which is the main difficulty in the interpretation of the photoemission data concerning the bulk band structure, is not a problem in the present case. In other words the results concerning the D_4 band are again independent of any assumption about the final bands and the discrepancy between theory and experiment must be a true effect.

A further interesting observation confirming the shift of the flat D_4 band comes from the dashed spectrum in Fig. 2. This EDC is collected from a nitrogen-contaminated surface. At these coverages ($\frac{1}{3}$ of a monolayer) the surface structure is $c(2\times2)$-N.[35] A comparison with the clean spectrum shows that distinct peaks appear at -2.0 and -4.5 eV as a result of nitrogen adsorption. Yet, the feature at -2.0 eV is not characteristic of nitrogen since we also observed it on Cr(100)-$c(2\times2)$-C and Cr(100)-$c(2\times2)$-S surfaces. We give a simple interpretation of the appearance of this structure in terms of surface umklapp processes: For a $c(2\times2)$ surface the $\bar{M}$ and $\bar{\Gamma}$ points of the (1×1) surface Brillouin zone become equivalent. Therefore, it can be seen from Fig. 1(a) that in normal photoemission bulk transitions may now be seen from the ΓH *and* PN symmetry lines which project on $\bar{\Gamma}$ and $\bar{M}$, respectively. The relevant surface umklapp process involves a surface reciprocal vector $\vec{G}_{||}$ at point $\bar{M}$. It explains

TABLE I. Occupied Cr band critical-point energies (eV) referred to the Fermi level.

Symmetry[a]	Experiment	GF[c]	LCGO[d]	LCGO[e]	MTB[f]
Γ'_{25} (Γ'_{25})	-0.95 ± 0.01[b]	-0.98 (-0.96)	-1.05	-0.90	-1.05
H_{12} (Γ_{12})	-3.40 ± 0.2	-4.39 (-4.36)	-4.00	-4.25	-3.30
N_1 (M_3)	-4.0 ±0.2	-4.26 (-4.24)	-4.27	-4.35	-3.90
N_2 (M_5)	-2.0 ±0.1	-2.46 (-2.42)	-2.60	-2.40	-2.45
P_4 (R'_{25})	-2.0 ±0.1	-2.18 (-2.28)	-2.28	-2.28	-2.05

[a]In parentheses is the symmetry of critical points for the perfect antiferromagnetic phase considered in Ref. 24.

[b]This value is extrapolated.

[c]Green's function (GF) method, Ref. 24. The values in parentheses correspond to the antiferromagnetic bands with the symmetry indicated in parentheses in the first column.

[d]Linear combination of Gaussian orbitals (LCGO), Ref. 29.

[e]Linear combination of Gaussian orbitals (Kohn-Sham-Gaspar exchange potential), Ref. 31.

[f]Modified tight-binding (MTB) and orthogonalized plane wave, Ref. 27.

the appearance of a peak at -2.0 eV in connection with the $c(2\times2)$ surface structure, as emission from the flat D_4 band.

Table I summarizes our experimentally determined critical-point energies obtained from $E(k)$ in Fig. 3. These measurements are compared to four different, self-consistent band calculations for paramagnetic Cr.[24,27,29,31] Values from the antiferromagnetic bands of Asano and Yamashita[24] are also shown for the relevant symmetry points in parentheses. The discrepancy with theory is typically 20% for N_2 and H_{12}. The calculations of Yasui *et al.*[27] are an exception since very good agreement is observed at H_{12} and P_4. Yet, similar discrepancies are observed in this case at N_2 and around the middle point of ΓH. Even larger d-band widths are reported from other calculations for either paramagnetic[28,30] or antiferromagnetic Cr.[25] The experimental energy of the Γ_{25}' point is the result of an extrapolation of our data concerning Δ_5. Good agreement is found here with the calculations as well as with the measurements of Johansson *et al.*[23] Actually, the narrowing of the d bands observed in photoemission gets support from optical-conductivity measurements.[45,46] Optical-conductivity calculations show peaks which correlate with experimental peaks, but which are shifted up in energy by almost 1 eV.[31] Since these features involve transitions between d-band states, it would also appear that the band calculations predict a too-large d-band width.

Finally, as to the magnetic-phase transition, let us point out that, excepting the surface-related features, the prominant peaks in the EDC's collected at room temperature can be interpreted as the result of direct transitions in the bcc Brillouin zone. In principle, since chromium is antiferromagnetic at room temperature, umklapp processes involving the wave vector Q of the spin-density wave should be visible in the form of additional structure in the spectra. In the approximation of perfect (commensurate) antiferromagnetism the Brillouin zone becomes that of a CsCl-type lattice. Thus, the Γ and H points become equivalent and, for instance, the bands along HN are folded back along ΓN. In particular, this signifies that in the spectra which probe points near H, structures should be seen which reflect emission from Bloch states near Γ. These features are apparently weak and therefore difficult to identify with certainty in our spectra. Possibly experiments at lower temperature might show them. In fact, since the perturbing spin-dependent potential which lowers the symmetry of the system in the magnetic state is quite small, these effects should be weak at most points of the Brillouin zone excepting the small regions where gaps are formed. Effects due to the magnetic-phase transition have been observed in photoemission[23] along the ΓM symmetry line where a gap is created in the antiferromagnetic phase.

IV. CONCLUSION

The experimentally determined band dispersions show a discrepancy with band calculations which increases with increasing binding energy. Whereas the agreement in good around -1 eV, the calculated binding energies are larger than measured at the bottom of the d band. At least for N_1, N_2, D_4, and P_4 this disagreement is not an artifact connected with the method used to interpret the photoemission data, based on the assumption of direct transitions to a free-electron-like final-state band. The observed discrepancies seem closely related to the d character of the bands. For instance, this can be seen in Fig. 3 for the D_4 band. The agreement with the calculations is better in the region where this band has not pure d character, i.e., near P_4 where p-d hybridization may occur than near N_2 which is a d-type $z(x$-$y)$ state. A similar statement holds for the lower Δ_1 band whose character changes from s to d because of s-d hybridization as one moves from Γ to H along ΓH. Notice also the better agreement at N_1, apparently because this state has non-negligible s character.

The present results again raise the question as to what extent the band-structure calculations properly include the exchange and correlation effects in metals with unfilled d bands. The similar compression of the d bands of Ni and Co has been explained by invoking correlation effects.[9–20] Possibly such effects are important in Cr too, though it is generally believed that the band (as opposed to quasiatomic) character of the d electrons is more pronounced in Cr than in Ni.[42,47] Note that evidence for the presence of a multielectron satellite has been reported.[23,42]

ACKNOWLEDGMENTS

The authors thank the members of the Laboratoire pour l'Utilisation du Rayonnement Electromagnétique for their help in the experiments using synchrotron radiation.

[1]F. J. Himpsel, J. A. Knapp, and D. E. A. Eastman, Phys. Rev. B 19, 2919 (1979).

[2]W. Eberhardt and E. W. Plummer, Phys. Rev. B 21, 3245 (1980).

[3]P. Heimann and H. Neddermeyer, J. Magn. Magn. Mater. 15-18, 1143 (1980).

[4]U. Gerhardt, C. J. Maetz, A. Schultz, and E. Dietz, J. Magn. Magn. Mater. 15-18, 1141 (1980).

[5]P. Thiry, D. Chandesris, J. Lecante, C. Guillot, R. Pinchaux, and Y. Petroff, Phys. Rev. Lett. 43, 82 (1979).
[6]J. Stohr, P. S. Wehner, R. S. Williams, G. Apai, and D. A. Shirley, Phys. Rev. B 17, 587 (1978).
[7]J. A. Knapp, F. J. Himpsel, and D. E. Eastmann, Phys. Rev. B 19, 4952 (1979).
[8]C. Guillot, Y. Ballu, J. Paigne, J. Lecante, K. P. Jain, P. Thiry, R. Pinchaux, Y. Petroff, and L. M. Falicov, Phys. Rev. Lett. 39, 1632 (1977).
[9]D. R. Penn, Phys. Rev. Lett. 42, 921 (1979).
[10]A. Liebsch, Phys. Rev. Lett. 43, 1431 (1979).
[11]A. Liebsch, Phys. Rev. B 23, 5203 (1981).
[12]L. C. Davis and L. A. Feldkamp, J. Appl. Phys. 50, 1944 (1979).
[13]L. C. Davis and L. A. Feldkamp, Solid State Commun. 34, 141 (1980).
[14]L. Kleinman, Phys. Rev. B 19, 1295 (1979).
[15]L. Kleinman, Phys. Rev. B 22, 6471 (1980).
[16]L. Kleinman and K. Mednick, Phys. Rev. B 24, 6880 (1981).
[17]G. Tréglia, F. Ducastelle, and D. Spanjaard, J. Phys. (Paris) 41, 281 (1980).
[18]G. Tréglia, F. Ducastelle, and D. Spanjaard, Phys. Rev. B 21, 3729 (1980).
[19]G. Tréglia, F. Ducastelle and D. Spanjaard, Phys. Rev. B 22, 6472 (1980).
[20]G. Tréglia, F. Ducastelle, and D. Spanjaard, J. Phys. (Paris) 43, 341 (1982).
[21]D. E. Eastman, F. J. Himpsel, and J. A. Knapp, Phys. Rev. Lett. 44, 95 (1980).
[22]A. M. Turner and J. L. Erskine, Phys. Rev. B 25, 1983 (1982).
[23]L. I. Johansson, L. G. Petersson, K. F. Berggren, and J. W. Allen, Phys. Rev. B 22, 3294 (1980).
[24]S. Asano and J. Yamashita, J. Phys. Soc. Jpn. 23, 714 (1967).
[25]H. L. Skriver, J. Phys. F 11, 97 (1981).
[26]M. Asdente and J. Friedel, Phys. Rev. 124, 384 (1961).
[27]M. Yasui, E. Hayashi, and M. Shimizu, J. Phys. Soc. Jpn. 29, 1446 (1970).
[28]R. P. Gupta and S. K. Sinha, Phys. Rev. B 3, 2401 (1971).
[29]J. Rath and J. Callaway, Phys. Rev. B 8, 5398 (1973).
[30]J. L. Fry, N. E. Brener, J. L. Thompson, and P. H. Dickinson, Phys. Rev. B 21, 384 (1980).
[31]D. G. Laurent, J. Callaway, J. L. Fry, and N. E. Brener, Phys. Rev. B 23, 4977 (1981).
[32]G. Gewinner, J. C. Peruchetti, R. Riedinger, and A. Jaéglé, Solid State Commun. 36, 785 (1980), and unpublished.
[33]G. Gewinner, J. C. Peruchetti, A. Jaéglé, and R. Riedinger, Phys. Rev. Lett. 43, 935 (1979).
[34]J. S. Foord and R. M. Lambert, Surf. Sci. 115, 141 (1982).
[35]G. Gewinner, J. C. Peruchetti, and A. Jaéglé, Surf. Sci. 122, 383 (1982).
[36]L. F. Wagner, Z. Hussain, and C. S. Fadley, Solid State Commun. 21, 257 (1977).
[37]T. C. Chiang, J. A. Knapp, M. Aono, and D. E. Eastman, Phys. Rev. B 21, 3513 (1980).
[38]G. D. Mahan, Phys. Rev. B 2, 4334 (1970).
[39]D. E. Eastman, F. J. Himpsel, J. A. Knapp, and K. C. Pandey, *Proceedings of the Fourteenth International Conference on the Physics of Semiconductors, Edinburgh, 1978,* edited by B. L. H. Wilson (IOP, Bristol, 1979), p. 1059.
[40]J. Hermanson, Solid State Commun. 22, 9 (1977).
[41]S. L. Weng, E. W. Plummer, and T. Gustafsson, Phys. Rev. B 18, 1718 (1978).
[42]J. Barth, F. Gerken, K. L. I. Kobayashi, J. H. Weaver, and B. Sonntag, J. Phys. C 13, 1369 (1980).
[43]A. Zunger, G. P. Kerker, and M. L. Cohen, Phys. Rev. B 20, 581 (1979).
[44]L. Ley, O. B. Dabbousi, S. P. Kowalczyk, F. R. McFeely, and D. A. Shirley, Phys. Rev. B 16, 5372 (1977).
[45]P. B. Johnson and R. W. Christy, Phys. Rev. B 9, 5056 (1974).
[46]J. E. Nestell, Jr., and R. W. Christy, Phys. Rev. B 21, 3173 (1980).
[47]Lo I. Yin, T. Tsang, and I. Adler, Phys. Rev. B 15, 2974 (1977).